A novel 4-phenyl amino thiourea derivative designed for real-time ratiometric–colorimetric detection of toxic Pb^{2+}

Yi S. Guang, Xia Ren, Shuang Zhao, Quan Z. Yan, Gang Zhao & Yao H. Xu

Published online: 16 Jan 2018.

Submit your article to this journal ↗

View related articles ↗

View Crossmark data ↗

Taylor & Francis
Taylor & Francis Group

Check for updates

A novel 4-phenyl amino thiourea derivative designed for real-time ratiometric–colorimetric detection of toxic Pb^{2+}

Yi S. Guang[a], Xia Ren[a,b], Shuang Zhao[b], Quan Z. Yan[a,c], Gang Zhao[a,b], and Yao H. Xu[a,b]

[a]School of Chemistry, Chemical Engineering and Biotechnology, Donghua University, Shanghai, China; [b]College of Materials Sciences and Engineering, Donghua University, Shanghai, China; [c]School of Chemistry and Chemical Engineering, Qufu Normal University, Qufu, China

ABSTRACT

The objective of this study was to develop a ratiometric and colorimetric organic sensor for Pb^{2+} detection in environmental samples. A new probe 4-phenyl amino thiourea (PAT) was designed and synthesized using hydrazine hydrate and phenyl isothiocyanate as raw materials. After its structure was characterized and confirmed, its UV–vis spectral property was investigated in detail. PAT possesses a specifically real-time, ratiometric and colorimetric response to Pb^{2+} in dimethyl formamide (DMF)/H_2O (v/v = 9:1, pH = 7.0) within 18.0 s. There was little interference in the presence of some other common metal ions, such as Fe^{3+}, Cd^{2+}, Zn^{2+}, Mg^{2+}, Cr^{3+}, Ca^{2+}, Ba^{2+}, Sn^{2+}, Na^+, Mn^{2+}, Hg^{2+}, and Pb^{2+}. Under the optimized conditions (DMF/H_2O with v/v of 9:1, $c_{PAT} = 1.0 \times 10^{-3}$ mol·L^{-1}, pH = 7.0), the present sensor PAT was successfully applied for Pb^{2+} determination in environmental water samples with satisfied recoveries (83.0%–106.0%) and analytical precision ($\leq$7.2%). The recognition mechanism was confirmed to form a stable 1:1 six-member ring complex between the target dye and Pb^{2+} with a coordination constant of 4.96×10^4.

Introduction

As one of the hottest topics in our society, environmental contamination by heavy metals has attracted more and more attention, along with the rapid development of modern industries, especially the development of modern mineral industry and electronic industry. Unscrupulous metal ions have been poured into the natural environment, which has made a major impact on people's health and lifestyle.[1–7] Among all the heavy metal ions, Pb^{2+} is the second most toxic and dangerous as it binds to sulfhydryl groups of enzymes, which affects almost every organ and system in human body through interfering with the proper functions and causing severe damages to the brain and kidneys, and ultimately this leads to death.[8–11] Accordingly, a convenient, rapid, sensitive and on-site detection of Pb^{2+} is of great importance.[12]

Although classic detection methods including atomic absorption spectrometry,[13,14] fluorescence spectrometry,[15–18] electrochemical techniques[19,20] and inductively coupled plasma-mass spectrometry[21] could detect Pb^{2+} with high selectivity and sensitivity, most of them required complicated instrumentation and cumbersome laboratory procedure. By virtue of its low testing cost, simple sensing process, and even to utilize naked eyes instead of the complex instrument, colorimetric methods have attracted more and more attention recently.[22–28] For example, Wang, et al.,[29] reported gold nanoparticles modified with DNAzyme as a label-free colorimetric probe for Pb^{2+} detection with a nanomolar detection limit and tunable dynamic range. The work developed a fast and simple label-free colorimetric sensor for on-site and real-time lead detection. Dwivedi, et al.,[30] developed a dithiothreitol functionalized anisotropic gold nanoparticles-based colorimetric sensor for detection of Pb^{2+} with good selectivity and sensitivity. By loading unmodified gold nanoparticles into poly(oligo(ethylene glycol)methacrylate) brushes, Ferhan, et al.,[31] for the first time, introduced a novel solid-phase colorimetric sensor for Pb^{2+} detection using metallic nanoparticles as a colorimetric sensing module. They were all at the expense of noble metal and their composites, however, simple and cheap organic small molecule-based ratiometric and colorimetric sensors for real-time determination Pb^{2+} have been less studied so far.

The objective of this study is to develop a ratiometric and colorimetric organic sensor for Pb^{2+} detection, which is expected to reduce the system error and to improve the sensitivity. Accordingly, a functional chemosensor, 4-phenyl amino thiourea (PAT), was identified and prepared using hydrazine hydrate and phenyl isothiocyanate as raw materials. PAT could effectively signal Pb^{2+} by virtue of the absorption peak at 342 nm decreasing and that at 393 nm increasing. A stable 1:1 six-member ring complex mechanism was proposed by means of UV–vis spectra titrations, ¹H NMR titrations, Job plot and binding constant. The present method was successfully applied in colorimetric detection of Pb^{2+} in environmental samples and the result has well met the requirement defined by the China Health Organization (CHO) in drinking water (GB/T 5750.6-2006).

CONTACT Yi S. Guang ✉ syg@dhu.edu.cn; Quan Z. Yan ✉ yanzhq2008@163.com; Yao H. Xu ✉ hongyaoxu@163.com School of Chemistry, Chemical Engineering and Biotechnology, Donghua University, Shanghai 201620, China.
Color versions of one or more of the figures in the article can be found online at www.tandfonline.com/lesa.

Materials and methods

Reagents and Apparatus

Hydrazine hydrate, phenyl isothiocyanate, 4-hydroxyethyl piperazine sulfonic acid (HEPES) and all the other chemicals were of AR grade and were used as received from Sinopharm Chemical Reagent Co. Ltd. Water used throughout was doubly deionized.

IR spectra were recorded on a Nicolet 8700 infrared spectrometer, mixed with KBr and pressed into pellets, scanned from 4,000–500 cm^{-1}. ^1H NMR was recorded using a Bruker AMX-393 spectrometer operating at 400 MHz, with tetramethyl-silane as a reference and dimethyl sulfoxide (DMSO)-d_6 as solvent. Elemental analysis was conducted using an Elemental Vario EL-III apparatus. Pb content in solution was determined using an inductively coupled plasma mass spectrometer (ICP-MS) (PerkinElmer, Elan DRC Plus). UV–vis spectra were recorded on a Shimadzu UV-265 spectrometer using a 1-cm square quartz cell. All pH measurements were made with a PHS-25 pH meter.

Preparations of the target probe (PAT)

To 1.2 mL (19.8 mmol) 80% hydrazine hydrate solution in 20 mL acetonitrile, 0.85 mL (19.8 mmol), phenyl isothiocyanate was added dropwise at room temperature and then the mixture was stirred and refluxed for 5 h at 82°C under N_2 atmosphere. After the reaction mixture was cooled to room temperature, the resultant precipitate was filtered and washed with enough acetonitrile, which was purified by recrystallization from acetone several times to provide white crystal (PAT) in the yield of 52.2%.

Fourier transform infrared spectroscopy (FTIR) (KBr), υ (cm^{-1}): 3321, 3116 (NH_2), 2061 (–N = C = S), 1192 (C = S), 1541 (C–N). ^1H-NMR (DMSO-d_6, 400 Hz) δ (ppm): 3.33 (s, 2H, NH_2), 7.16–7.55 (m, J = 8.5 Hz, 5H, ArH); 9.64–9.87 (d, J = 5.6 Hz, 2H, NH). Anal. Calcd for $C_7H_9N_3S$ (%): C 50.28, H 5.43, N 25.13; Found: C 50.30, H 5.39, N 25.17.

Procedures of detection

For Pb^{2+} detection, 1.0 mL HEPES buffer solution (pH 7.0), 1.0 mL 1.0×10^{-3} $mol·L^{-1}$ PAT in N,N-dimethyl formamide (DMF) and 1.0 mL Pb^{2+} solution with different concentrations were transferred into a 10 mL volumetric flask. The mixture was diluted to 10 mL with DMF. After incubating for 1.0 min, the absorption spectra were recorded and the band-slit was set as 2.0 nm. The ratio ($A_{393/342}$) of the absorption intensity at 393 nm to that at 342 nm was used for quantitative analysis.

Results and discussion

The UV–vis absorption spectrum of PAT

To confirm its spectral performance and potential application, the UV–vis absorption spectra of PAT were tested first in the absence and presence of Pb^{2+} in DMF/H_2O (v/v = 9:1, pH 7.0) and the results were given in Figure 1. From Figure 1 we could find that PAT itself possesses two absorption peaks at 274 nm
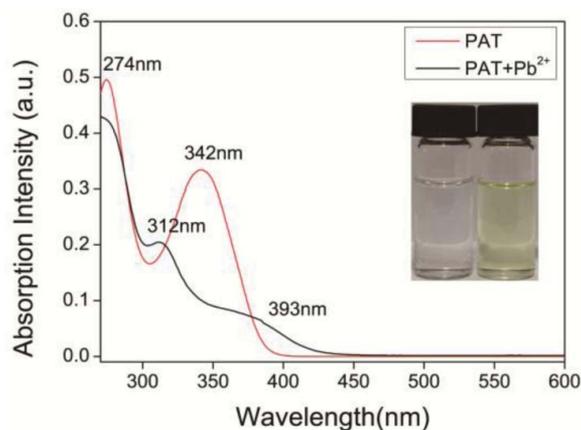

Figure 1. UV–vis absorption spectra of PAT in the absence and presence of Pb^{2+} in DMF/H_2O (v/v = 9:1, $c_{Pb}^{2+} = 5.0 \times 10^{-5}$ $mol·L^{-1}$, pH = 7.0; $c_{PAT} = 1.0 \times 10^{-3}$ $mol·L^{-1}$).

and 342 nm in DMF/H_2O (v/v = 9:1, pH = 7.0). The first absorption peak at 274 nm is attributed to the π–π electron transition of phenyl ring moiety, and the second at 342 nm results from the π–π electron transition of C = S bond, an auxochrome group conjugated to phenyl ring with ε_{max} of 3.4×10^4 $L·mol^{-1}·cm^{-1}$. Once upon addition of Pb^{2+}, the absorbance at 342 nm disappeared eventually with the emergence of two new absorption peaks at 312 nm and 393 nm, respectively. Importantly, the color of the solution changed from colorless to light yellow, which made it possible for naked-eye detection of Pb^{2+}. An absorption peak shifted to long wavelength suggests that a better rigid configuration formed for PAT in the presence of Pb^{2+}.

Effect of water-content

To make sure that the proposed probe could be applied in aqueous environment, the effect of water-content on the absorption spectra was investigated in the absence and presence of Pb^{2+} (Figure 2). From Figure 2, we could find that there is little effect of water-content on the ratio ($A_{393/342}$) without Pb^{2+}, implying that PAT itself is quite stable. While in the presence of Pb^{2+}, $A_{393/342}$ reaches the maximum at 10% water (v/v)
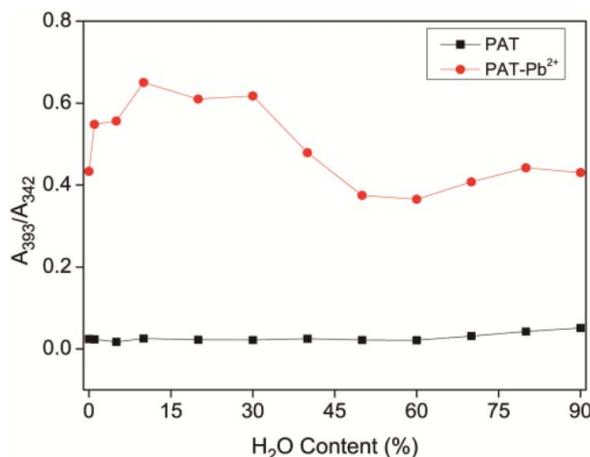

Figure 2. The effect of water-content on the absorption spectra of PAT in the absence and presence of Pb^{2+}, respectively.
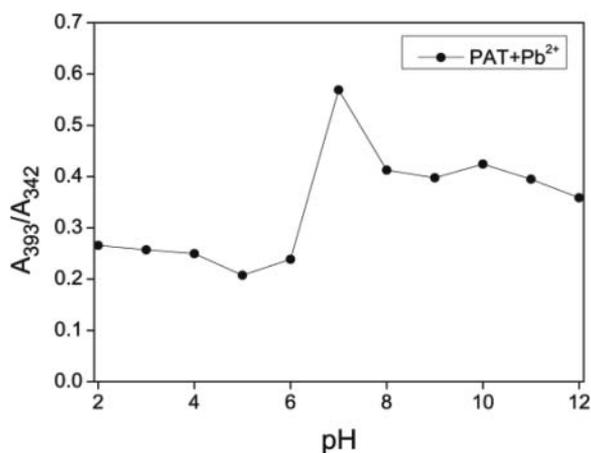
Figure 3. Effect of pH on $A_{393/342}$ of PHT-Pb^{2+} in DMF/H_2O (v/v = 9:1, c_{Pb}^{2+} = 5.0 × 10^{-5} mol·L^{-1}, c_{PAT} = 1.0 × 10^{-3} mol·L^{-1}).

Figure 4. Time response curve of PAT to Pb^{2+} in DMF/H_2O (v/v = 9:1, c_{Pb}^{2+} = 5.0 × 10^{-5} mol·L^{-1}, c_{PAT} = 1.0 × 10^{-3} mol·L^{-1}, pH = 7.0); Inset: the amplified curve of the response of PAT to Pb^{2+} between 0 and 30.0 s.

and then decreases more than 10% water (v/v). The reason may be that protic H_2O could form strong hydrogen bonding with PAT, which will enhance the conjugated degree to improve the absorption intensity.[32,33] Once the H_2O content was more than 10%, protic H_2O would thus compete with PAT to bind Pb^{2+}, which will reduce the chance of complexation between PAT and Pb^{2+}. DMF/H_2O (v/v = 9:1) was selected for all subsequent experiment in the work accordingly.

Effect of pH

As a protic amino-based colorimetric probe, pH will possess a significant influence on the interaction between PAT and Pb^{2+}, the effect of pH on the detection was measured in the range of pH 2.0–12.0 (Fig. 3). $A_{393/342}$ gradually first increases with pH and reaches the maximum when pH is 7.0. The reason might be that when pH is <7.0, both N and S atoms in PAT molecule are easily protonated, which reduces their coordination with Pb^{2+}. While pH is more than 7.0, the solubility of Pb^{2+} in basic aqueous solution decreases. They both attenuate the coordination interaction between PAT and Pb^{2+}, resulting in decrease of $A_{393/342}$. Accordingly, pH 7.0 was selected for all the subsequent experiments in the work.

Time response

To illustrate the response rate and reliability of PAT to recognize Pb^{2+}, $A_{393/342}$ of PHT-based sensing system in DMF/H_2O (v/v = 9:1, c_{Pb}^{2+} = 5.0 × 10^{-5} mol·L^{-1}, c_{PAT} = 1.0 × 10^{-3} mol·L^{-1}) was measured at different times after addition of Pb^{2+}. It is easy to find from Figure 4 that $A_{393/342}$ increases quickly and could reach a platform within less than 18.0 s after addition of Pb^{2+} (Inset in Fig. 4). To the best of our knowledge, it may be so far one of the fastest real-time Pb^{2+}-quantification assays achieved at room temperature at pH 7.0 using an organic colorimetric probe. Furthermore, the absorption spectral signals can remain stable during the subsequent test time, implying that the proposed PAT-based colorimetric probe is sensitive, and possesses fast real-time response, reliability and stability.
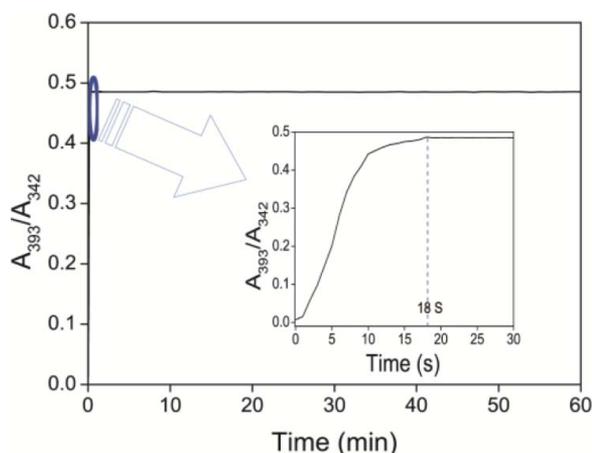
Effect of coexisting foreign metal ions

To illustrate the selectivity of PAT-based sensing system for Pb^{2+} detection, the colorimetric response of PAT to Pb^{2+} was compared to other environmentally important metal ions, such as Fe^{3+}, Cd^{2+}, Zn^{2+}, Mg^{2+}, Cr^{3+}, Ca^{2+}, Ba^{2+}, Sn^{2+}, Na^+, Mn^{2+}, and Hg^{2+}. For this, the relative values of $A_{393/342}$ of the sensing system containing 5.0 × 10^{-5} mol·L^{-1} Pb^{2+} and 1.0 × 10^{-5} mol·L^{-1} PAT at pH 7.0 were recorded in the absence and presence of other different metal ions above (Fig. 5). From Figure 5, we could find that the additions of these metal ions show negligible effect on $A_{393/342}$ of the proposed sensing system, i.e., all the changes are less than 5% relative to that taken in the presence of Pb^{2+} under the same conditions. The selectivity of PAT to Pb^{2+} detection is excellent, which could be applied for colorimetric detection of Pb^{2+}, even under the condition of coexistence of other metal ions.

Analytical parameters and application in practice

To disclose the rule of PAT for colorimetric detection of Pb^{2+}, series of UV–vis spectral titration experiments were carried out
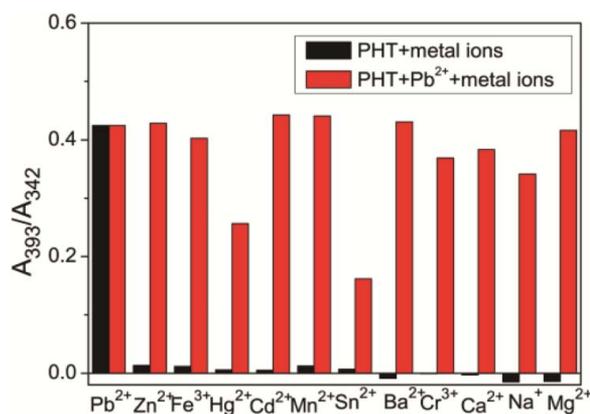

Figure 5. The relative absorption responses of the PAT sensing system in the presence of various metal ions. Black bars represent the addition of various metal ion to PAT. The magenta bars represent the addition of various metal ion to PAT-Pb^{2+} (v/v = 9:1, c_{Pb}^{2+} = 5.0 × 10^{-5} mol·L^{-1}, $c_{other\ ion}$ = 1.0 × 10^{-4} mol·L^{-1}, c_{PAT} = 1.0 × 10^{-3} mol·L^{-1}, pH = 7.0).
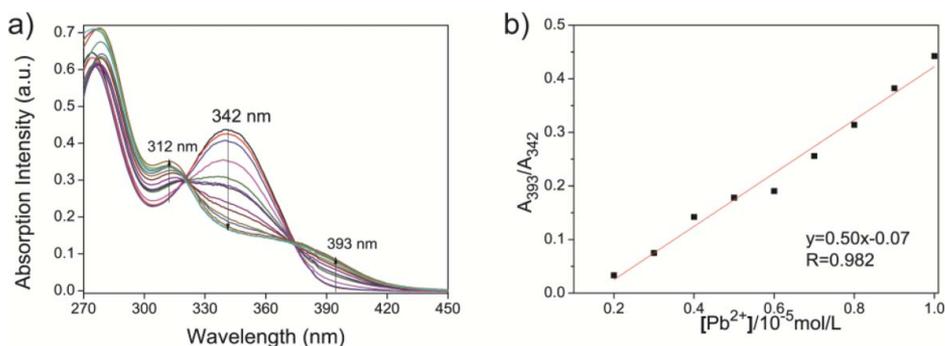
Figure 6. a) The UV-Vis absorption spectra of PAT (1.0×10^{-5} M) upon addition of Pb^{2+} (0–50 μM) in DMF/H$_2$O (9/1, v/v, pH = 7.0). b) The linear relationship between $A_{393/342}$ and c_{Pb}^{2+}.

under the given optimized experimental conditions. Figure 6 shows the absorption spectra of PAT at different concentrations of Pb^{2+} between 0 mol·L^{-1} and 5.0×10^{-6} mol·L^{-1}. From the spectra, a linear relationship between PAT and Pb^{2+} concentration is exhibited in the range of $2.0–10.0 \times 10^{-6}$ mol·L^{-1} with a correlation coefficient of 0.982. The regression equation is $A_{393/342} = -0.07 + 0.5 c$ (10^{-6} mol·L^{-1}). Based on the definition of detection limit, three times of the average deviation of absorbing intensity ratio ($A_{393/342}$) of the intensity at 393 nm to that at 342 nm in 20 blank samples without Pb^{2+} being used here, the limit of detection for Pb^{2+} is up to 2.3×10^{-7} mol·L^{-1}, which well meets the concentration limits defined by the China Health Organization (CHO) in drinking water (GB/T 5750.6-2006).

To further evaluate the feasibility, the proposed PAT-based sensing system has been applied to analyse four environmental water samples from the Lake, the tap water on the campus and the untreated industrial wastewater from the battery plant at Baoshan district in Shanghai, respectively (Table 1). All the samples were obtained by filtering several times. For recovery studies, some known concentrations of Pb^{2+} were added to the environmental water samples and the total Pb^{2+} concentration was determined following the method proposed above. From Table 1, we could find that the recoveries of different known amounts of Pb^{2+} spiked were obtained from 83.0% to 106.0% with a satisfying analytical precision (R.S.D. ≤ 7.2%). Especially, the detected values in the samples were quite consistent with the ones obtained from ICP-MS, which validated the reliability and practicality of this method for Pb^{2+} detection.

The recognition mechanism

It is well known that Job's plot is one of the most popular methods to determinate stoichiometry in host–guest chemistry.[34] To investigate the action mechanism between PAT and Pb^{2+},

Job's plot was drawn first. To do this, a series of solutions with varying mole fraction of Pb^{2+} to PAT were prepared by maintaining the total concentration constant of 1.0×10^{-4} mol·L^{-1}. The absorption intensity at 393 nm was recorded for each solution (Fig. 7a). From Figure 7a, we could find that the observed maximum in the Job's plot is 0.5. So a 1:1 stoichiometry for the complex between PAT and Pb^{2+} was concluded, confirming that Pb^{2+} might simultaneously coordinate with N and S atoms in the target probe. Accordingly, a stable six-member ring coordination mode was proposed as schematized in Figure 7b.

Based on the proposed recognition mode between PAT and Pb^{2+}, the linear relationship between the reciprocal of relative absorption intensity [$1/A–A_0$] and the reciprocal of c_{Pb}^{2+} was drawn according to Benesi-Hildebrand formula below (Fig. 7a)[35]

$$1/(A - A_0) = 1/\{K_{a|} * (A_{max} - A_0) * [Pb^{2+}]\} + 1/(A_{max} - A_0)$$

where A and A_0 are the absorption intensity at 393 nm without and in the absence of Pb^{2+}, respectively. A_{max} is the maxima absorption intensity changed at 393 nm in the presence of Pb^{2+}. The binding constant (K_a) of PAT and Pb^{2+} was calculated to be 4.96×10^4, indicating that PAT could selectively recognize Pb^{2+} and the resultant complex PAT-Pb^{2+} is quite stable.

^{1}H NMR titrations were carried out to further discover the bonding nature between PAT and Pb^{2+} in the absence and presence of Pb^{2+} in DMF-d_6, and the results were shown in Figure 8. In the absence of Pb^{2+}, PAT possesses three N-H signals at 10.2 (position 4), 9.6 (position 5) and 3.5 (position 6) ppm, respectively. With gradual addition of Pb^{2+} from 0.0, 0.25, 0.50, 0.75 and 1.0 equivalent, all the three characterized signals, especially the signal at 3.5 ppm, shift to low field by 0.14, 0.20, 0.21 ppm, respectively. And no shift happens when Pb^{2+} is more than 1.0, i.e., 1.50 and 2.0 equivalents. On the

Table 1. Pb^{2+} colorimetric determination results for environmental samples ($n = 5$)[a].

Samples	c_{Pb}^{2+} in samples (10^{-6} M)	Spiked (10^{-6} M)	Found (10^{-6} M)	Recovery (%)	R.S.D. (%)	c_{Pb} by ICP-MS (10^{-6} M)
Lake water 1	0	5.0	4.87	97	6.9	4.98
Lake water 2	0	8.0	7.16	83	7.0	8.02
Tap water 1	0	5.0	5.2	104	3.2	5.01
Tap water 2	0	8.0	7.4	93	5.0	8.03
Wastewater 1	2.05	5.0	7.12	101	4.8	7.21
Wastewater 2	2.02	8.0	10.62	106	7.2	10.53

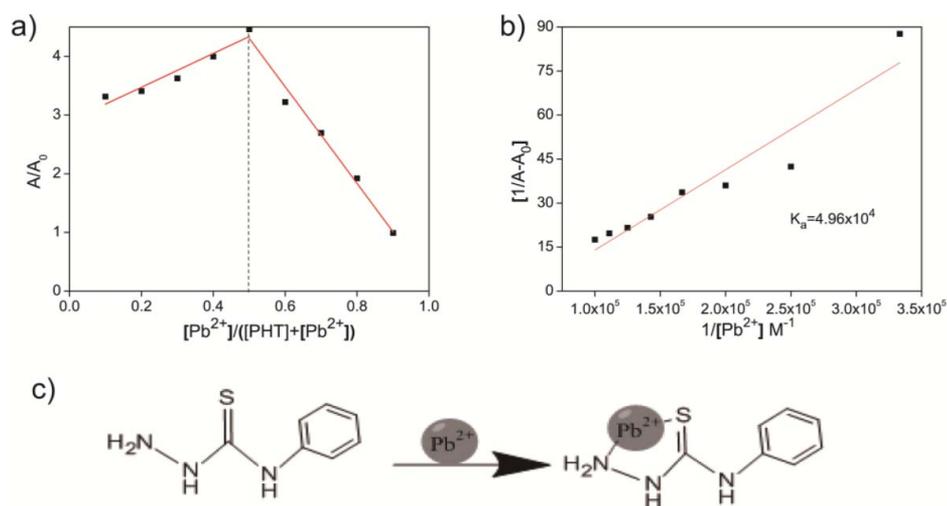[a]HEPES buffer solution (pH 7.0), $c_{PAT} = 1.0 \times 10^{-5}$ mol/L in DMF/H$_2$O (9/1, v/v, pH = 7.0).

Figure 7. a) Job-plot for PAT and Pb^{2+}, the total concentration of PAT and Pb^{2+} kept at 100 μmol/L. b) The proposed recognition mode of PAT to Pb^{2+}. c) A certain linear relationship between $1/[A-A_0]$ and $1/[Pb^{2+}]$.
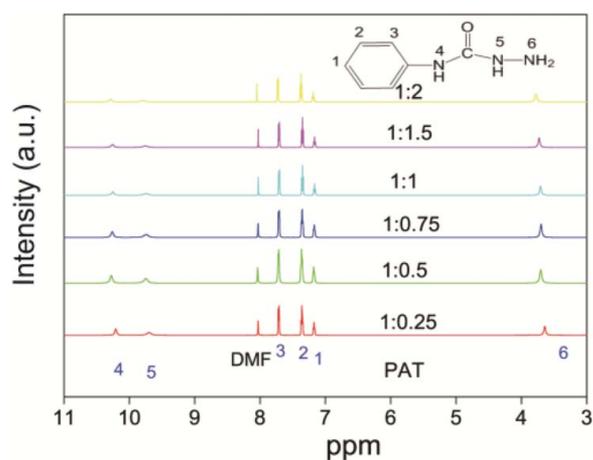

Figure 8. Partial ^{1}H NMR spectra of PAT in DMF-d_7 upon addition of Pb^{2+}. [PAT] = 1.0×10^{-3} M.

other hand, there are no δ shifts found for other H atoms. The results further confirmed that Pb^{2+} coordinated simultaneously with N and S atoms in the target probe by 1:1 stoichiometry as proposed above (Fig. 7c).

Conclusion

In conclusion, a novel ratiometric colorimetric sensor, PAT, was designed and demonstrated for the detection of Pb^{2+} in DMF/H_2O (v/v = 9:1, $c_{PAT} = 1.0 \times 10^{-3}$ mol·L^{-1}, pH = 7.0). PAT displays excellent selectivity for Pb^{2+} due to the special sulfur affinity nature, which could simultaneously coordinate with N and S atoms to form a stable six-member ring. Under the optimized conditions, the proposed method could real-timely recognize Pb^{2+} within 18.0 s with a linear range of $2.0-10.0 \times 10^{-6}$ mol·L^{-1} and a correlation coefficient of 0.982. The limit of detection was up to 2.3×10^{-7} mol·L^{-1}, which meets the requirement defined by the CHO in drinking water (GB/T 5750.6-2006). The presented method has been applied successfully to the determination of Pb^{2+} in environmental samples with satisfied recoveries (83.0%–106.0%) and analytical

precision ($\leq$7.2%). A potential ratiometric and colorimetric sensor was presented for real-time recognition of Pb^{2+} with excellent selectivity and sensitivity.

Funding

References

[1] Alshahri, F. Heavy metal contamination in sand and sediments near to disposal site of reject brine from desalination plant, Arabian Gulf: Assessment of environmental pollution. *Environ. Sci. Pollut. R. Int.* **2017**, *24*, 1821–1831. doi:10.1007/s11356-016-7961-x.

[2] Zhang, Z. Y.; Abuduwaili, J.; Jiang, F. Q. Heavy metal contamination, sources, and pollution assessment of surface water in the Tianshan Mountains of China. *Environ. Monit. Assess.* **2015**, *187*, 33. doi:10.1007/s10661-014-4191-x.

[3] Dong, X. Q.; Li, C. L.; Li, J.; Wang, J. X.; Liu, S. T.; Ye, B. A novel approach for soil contamination assessment from heavy metal pollution: A linkage between discharge and adsorption. *J. Hazard. Mater.* **2010**, *175*, 1022–1030. doi:10.1016/j.jhazmat.2009.10.112.

[4] Yan, Z. Q.; Zhao, Q.; Wen, M. J.; Hu, L.; Zhang, X. Z.; You, J. M. A novel polydentate ligand chromophore for simultaneously colorimetric detection of trace Ag^+ and Fe3+. *Spectrochim. Acta, Part A.* **2017**, *186*, 17–22. doi:10.1016/j.saa.2017.06.007.

[5] Guang, S. Y.; Tian, J. C.; Wei, G.; Yan, Z. Q.; Pan, H. F.; Feng, J. H.; Xu, H. Y. A modified fluorescein derivative with improved water-solubility for turn-on fluorescent determination of Hg^{2+} in aqueous and living cells. *Talanta.* **2017**, *170*, 89–96. doi:10.1016/j.talanta.2017.03.108.

[6] Yan, Z. Q.; Hu, L.; You, J. M. Sensing materials developed and applied for bio-active Fe^{3+} recognition in water environment. *Anal. Methods* **2016**, *8*, 5738–5754. doi:10.1039/C6AY01502F.

[7] Kim, H. N.; Ren, W. X.; Kim, J. S.; Yoon, J. Fluorescent and colorimetric sensors for detection of lead, cadmium, and mercury ions. *Chem. Soc. Rev.* **2012**, *41*, 3210–3244. doi:10.1039/C1CS15245A.

[8] Gondal, M. A.; Dastageer, M. A.; Al-Adel, F. F.; Naqvi, A. A.; Habibullah, Y. B. Detection of highly toxic elements (lead and chromium) in commercially available eyeliner (kohl) using laser induced break down spectroscopy. *Opt. Laser Technol.* **2015**, *75*, 99–104. doi:10.1016/j.optlastec.2015.06.024.

[9] Awual, M. R.; Hasan, M. M. Novel conjugate adsorbent for visual detection and removal of toxic lead(II) ions from water.

Microporous Mesoporous Mater. **2014,** *196,* 261–269. doi:10.1016/j.micromeso.2014.05.021.

[10] Gondal, M. A.; Dastageer, M. A.; Naqvi, A. A.; Isab, A. A.; Maganda, Y. W. Detection of toxic metals (lead and chromium) in talcum powder using laser induced breakdown spectroscopy. *Appl. Opt.* **2012,** *51,* 7395–7401. doi:10.1364/AO.51.007395.

[11] Ha, X. Q.; Yin, Q.; Lu, T. D.; Liu, B.; Xu, Y. B.; Liu, C. J.; Yu, X. H. Lead acetate in drinking water is toxic to hippocampal tissue Measuring relative protein changes using tissue array detection. *Neural Regener. Res.* **2010,** *5,* 519–524.

[12] Jiang, J.; Li, S. Q.; Yan, Y. X.; Fang, M.; Chen, M.; Peng, K.; Nie, L. F.; Feng, Y.; Wang, X. Pendant structure governed the selectivity of Pd^{2+} using disubstituted polyacetylenes with sulfur functions and the application of thiophanate-methyl detection. *Sens. Actuators, B* **2017,** *247,* 36–45. doi:10.1016/j.snb.2017.03.008.

[13] Chen, W.; Xiong, Q. X.; Pang, X. F.; Zhu, X. P.; Han, M.; Zhao, Q. X.; Liu, W. H. Study of adsorption and desorption of behaviors of Pb^{2+} on thiol-modified bentonite by flame atomic absorption spectrometry. *Spectrosc. Spect. Anal.* **2013,** *33,* 817–821.

[14] Tarley, C. R. T.; Andrade, F. N.; de Oliveira, F. M.; Corazza, M. Z.; de Azevedo, L. F. M.; Segatelli, M. G. Synthesis and application of imprinted polyvinylimidazole-silica hybrid copolymer for Pb^{2+} determination by flow-injection thermospray flame furnace atomic absorption spectrometry. *Anal. Chim. Acta.* **2011,** *703,* 145–151. doi:10.1016/j.aca.2011.07.029.

[15] Wan, J.; Zhang, K.; Li, C.; Li, Y. Y.; Niu, S. Y. A novel fluorescent chemosensor based on a rhodamine 6G derivative for the detection of Pb^{2+} ion. *Sens. Actuators, B* **2017,** *246,* 696–702. doi:10.1016/j.snb.2017.02.126.

[16] Bian, R. X.; Wu, X. T.; Chai, F.; Li, L.; Zhang, L. Y.; Wang, T. T.; Wang, C. G.; Su, Z. M. Facile preparation of fluorescent Au nanoclusters-based test papers for recyclable detection of Hg^{2+} and Pb2+. *Sens. Actuators, B* **2017,** *241,* 592–600. doi:10.1016/j.snb.2016.10.120.

[17] Zhao, M. L.; Zhou, X. F.; Tang, J.; Deng, Z. F.; Xu, X.; Chen, Z.; Li, X. T.; Yang, L. T.; Ma, L. J. Pyrene excimer-based fluorescent sensor for detection and removal of Fe^{3+} and Pb^{2+} from aqueous solutions. *Spectrochim. Acta, Part A* **2017,** *173,* 235–240. doi:10.1016/j.saa.2016.09.033.

[18] Xiang, Y.; Tong, A. J.; Lu, Y. A basic site-containing DNAzyme and aptamer for label-free fluorescent detection of Pb^{2+} and adenosine with high sensitivity, selectivity, and tunable dynamic range. *J. Am. Chem. Soc.* **2009,** *131,* 15352–15357. doi:10.1021/ja905854a.

[19] Sun, Q. W.; Wang, J. K.; Tang, M. H.; Huang, L. M.; Zhang, Z. Y.; Liu, C.; Lu, X. H.; Hunter, K. W.; Chen, G. S. A new electrochemical system based on a flow-field shaped solid electrode and 3D-printed thin-layer flow cell: Detection of Pb^{2+} ions by continuous flow accumulation square-wave anodic stripping voltammetry. *Anal. Chem.* **2017,** *89,* 5024–5029. doi:10.1021/acs.analchem.7b00383.

[20] Zhu, Y.; Zeng, G. M.; Zhang, Y.; Tang, L.; Chen, J.; Cheng, M.; Zhang, L. H.; He, L.; Guo, Y.; He, X. X. Highly sensitive electrochemical sensor using a MWCNTs/GNPs-modified electrode for lead (II) detection based on Pb^{2+}-induced G-rich DNA conformation. *Analyst* **2014,** *139,* 5014–5020. doi:10.1039/C4AN00874J.

[21] Saito, E.; Antunes, E. F.; Zanin, H.; Marciano, F. R.; Lobo, A. O.; Trava-Airoldi, V. J.; Corat, E. J. Oxygen plasma exfoliated vertically-aligned carbon nanotubes as electrodes for ultrasensitive stripping detection of Pb2+. *J. Electrochem. Soc.* **2014,** *161,* H321–H325. doi:10.1149/2.039405jes.

[22] Nie, L.; Zhang, Q.; Hu, L.; Liu, Y. M.; Yan, Z. Q. Modified hydrazone derivatives for ratiometric and colorimetric recognition of F^-: Relationship between architecture and performances. *Sens. Actuators, B* **2017,** *245,* 314–320. doi:10.1016/j.snb.2017.01.152.

[23] Yan, Z. Q.; Hu, L.; Nie, L.; You, J. M. One-pot preparation of graphene-Ag nano composite for selective and environmentally-friendly recognition of trace mercury(II). *RSC Adv.* **2016,** *6,* 109857–109861. doi:10.1039/C6RA16810H.

[24] Yan, Z. Q.; Xue, H. T.; Berning, K.; Lam, Y. W.; Lee, C. S. Identification of multifunctional graphene-gold nanocomposite for environment-friendly enriching, separating, and detecting Hg^{2+} simultaneously. *ACS Appl. Mater. Interfaces* **2014,** *6,* 22761–22768. doi:10.1021/am506875t.

[25] Yu, Y. M.; Hong, Y.; Gao, P.; Nazeeruddin, M. K. Glutathione modified gold nanoparticles for sensitive colorimetric detection of Pb^{2+} ions in rainwater polluted by leaking perovskite solar cells. *Anal. Chem.* **2016,** *88,* 12316–12322. doi:10.1021/acs.analchem.6b03515.

[26] Yun, W.; Cai, D. Z.; Jiang, J. L.; Zhao, P. X.; Huang, Y.; Sang, G. Enzyme-free and label-free ultra-sensitive colorimetric detection of Pb^{2+} using molecular beacon and DNAzyme based amplification strategy. *Biosens. Bioelectron.* **2016,** *80,* 187–193. doi:10.1016/j.bios.2016.01.053.

[27] Shi, X. H.; Gu, W.; Zhang, C. L.; Zhao, L. Y.; Peng, W. D.; Xian, Y. Z. A label-free colorimetric sensor for Pb^{2+} detection based on the acceleration of gold leaching by graphene oxide. *Dalton Trans.* **2015,** *44,* 4623–4629. doi:10.1039/C4DT03883E.

[28] Chen, H. B.; Sun, H. X.; Zhang, X. F.; Sun, X. R.; Shi, Y. H.; Tang, Y. L. A supramolecular probe for colorimetric detection of Pb^{2+} based on recognition of G-quadruplex. *RSC Adv.* **2015,** *5,* 1730–1734. doi:10.1039/C4RA11395K.

[29] Wang, Z. D.; Lee, J. H.; Lu, Y. Label-free colorimetric detection of lead ions with a nanomolar detection limit and tunable dynamic range by using gold nanoparticles and DNAzyme. *Adv. Mater.* **2008,** *20,* 3263–3269. doi:10.1002/adma.200703181.

[30] Dwivedi, C.; Chaudhary, A.; Gupta, A.; Nandi, C. K. Direct visualization of lead corona and its nanomolar colorimetric detection using anisotropic gold nanoparticles. *ACS Appl. Mater. Interfaces* **2015,** *7,* 5039–5044. doi:10.1021/am507495j.

[31] Ferhan, A. R.; Guo, L. H.; Zhou, X. D.; Chen, P.; Hong, S.; Kim, D. H. Solid-phase colorimetric sensor based on gold nanoparticle-loaded polymer brushes: Lead detection as a case study. *Anal. Chem.* **2013,** *85,* 4094–4099. doi:10.1021/ac4001817.

[32] Yan, Z. Q.; Zhu, Y. J.; Xu, J.; Wang, C.; Zheng, Y. Y.; Li, P. Y.; Hu, L.; You, J. M. A novel polydentate Schiff-base derivative developed for multi-wavelength colorimetric differentiation of trace Fe^{2+} from Fe3+. *Anal. Methods.* **2017,** *9,* 6240–6245. doi:10.1039/C7AY02167D.

[33] Yan, Z. Q.; Li, Y. Z.; Gao, Y.; Wen, J. H.; Hu, L.; You, J. M. A rigid and planar D-π-A conjugated azo-derivative with long-wavelength absorption colorimetric determination of trace Fe(II). *Optic. Mater.* **2017,** *73,* 393–399. doi:10.1016/j.optmat.2017.08.048.

[34] Hibbert, D. B.; Thordarson, P. The death of the Job plot, transparency, open science and online tools, uncertainty estimation methods and other developments in supramolecular chemistry data analysis. *Chem. Commun.* **2016,** *52,* 12792–12805. doi:10.1039/C6CC03888C.

[35] Guo, D.; Dong, Z. P.; Luo, C.; Zan, W. Y.; Yan, S. Q.; Yao, X. J. A rhodamine B-based "turn-on" fluorescent sensor for detecting Cu^{2+} and sulfur anions in aqueous media. *RSC Adv.* **2014,** *4,* 5718–5725. doi:10.1039/c3ra45931d.